Journal of Engineering Management and Systems Engineering
https://www.acadlore.com/journals/JEMSE

Optimization of the Plasma Arc Cutting Process Through Technological Forecasting

Miloš Milovančević[1*], Kamen Boyanov Spasov[2], Abouzar Rahimi[3]

[1] Faculty of Mechanical Engineering, University of Niš, 18000 Niš, Serbia
[2] Faculty of Economics and Business Administration, University St. Kliment Ohridski, 1000 Sofia, Bulgaria
[3] Department of Civil Engineering, Islamic Azad University, 51368 Tabriz, Iran

* Correspondence: Miloš Milovančević (milovancevic@masfak.ni.ac.rs)

Received: 12-15-2023 **Revised:** 01-20-2024 **Accepted:** 01-26-2024

Citation: M. Milovančević, K. B. Spasov, and A. Rahimi, "Optimization of the plasma arc cutting process through technological forecasting ," *J. Eng. Manag. Syst. Eng.*, vol. 3, no. 1, pp. 30–37, 2024. https://doi.org/10.56578/jemse030103.

Abstract: This research employs a data-driven approach to optimize the plasma arc cutting process. The evaluation of cut quality is based on six output characteristics, while the input parameters include stand-off distance, cutting current, and cutting speed. The output metrics consist of the material removal rate (MRR), surface roughness, bevel angle, slag formation, kerf width, and heat-affected zone (HAZ). Given the complexity of the process and the multitude of involved processing parameters, it is imperative to develop an optimization model to ensure the production of undisturbed structures. The primary aim of this study is to identify the most critical factors that facilitate optimal conditions for plasma arc cutting. The research goal is to determine the influence of input parameters on the plasma arc cutting quality using an adaptive neural fuzzy inference system (ANFIS). It has been found that the material removal rate (MRR), surface roughness, bevel angle, slag formation, kerf width, and heat-affected zone (HAZ) are predominantly affected by the interplay of cutting current and stand-off distance. Ideally, the best predictive model for various attributes, such as MRR, bevel angle, slag formation, surface roughness, kerf width, and HAZ, is one that synergistically combines cutting current and stand-off distance. This study, which evaluates multiple input parameters simultaneously, is expected to attract significant attention as it represents a pioneering small-scale investigation in the field.

Keywords: Plasma arc cutting; Technology forecasting; Adaptive neural fuzzy inference system

1 Introduction

Despite the extensive application of plasma arc cutting (PAC) in heavy-duty manufacturing cycles, there are challenges and drawbacks that require careful consideration prior to its implementation. Traditional control methods falter due to the unique nature of the input parameters, necessitating advanced technological approaches for process enhancement.

PAC is renowned for its efficiency and versatility in cutting a wide range of materials within the industrial sector. A significant hurdle for PAC is the formation of dross [1]. The primary influential factors in the PAC process are identified as arc current, standoff distance, and cutting speed [2], with each factor carrying varying degrees of significance. A study on the heat-affected zone (HAZ) generated during PAC of stainless steel (Grade 304) revealed optimal cutting conditions utilizing response surface methodology (RSM): a voltage of 240 volts, a current of 65 amps, and a speed of 1.5 millimeters per second [3]. Employing these input parameters resulted in an output of a material removal rate (MRR) of 5.79 millimeters per second over a period of 246 seconds, achieving a surface roughness of 65 micrometers [4]. Analysis of the cut surface's microstructure uncovered the presence of a recast layer, microstriations, and dross accumulation [5]. Experimental results indicate that the proposed control method surpasses traditional PI control in enhancing accuracy, finish, ripple reduction, and overall quality of the workpiece, alongside other comprehensive metrics. Additionally, the power supply for PAC demonstrates exceptional control performance, attributed to its fuzzy-neural network framework [6].

The primary objective of this study is to pinpoint the variables that significantly influence the PAC process when applied to stainless steel [7]. The investigation proceeds through the evaluation and application of six distinctive

output characteristics. The adaptive neurofuzzy inference system (ANFIS) [8–10] is an extraordinarily effective tool for identifying and categorizing critical input parameters essential to the progression of the PAC process. This system is characterized by robustness, resilience, immunity to interference, fault tolerance, conformity with ANFIS standards, and proficiency in normalization and generalization. Consequently, variations in the characteristics are unlikely to significantly impact the performance of the PAC method as refined by ANFIS [11–13].

2 Methodology

2.1 Experimental Setup and Data

To conduct the cutting tests, stainless steel AISI 304 specimens measuring 250×70×50mm were prepared. The input parameters include standoff distance, cutting current, and cutting speed. The outputs, such as material removal rate (MRR), chamfer, surface roughness, dross, kerf width, and heat-affected zone (HAZ), are measured. The MRR is efficiently determined using electronic weighing equipment. Surface roughness is assessed with a Talysurf instrument, while the remaining outputs are measured using an automated Vernier caliper. Figure 1 displays the experimental setup of the plasma arc cutting system. Table 1 presents sample experimental data related to the input and output variables [14–16].

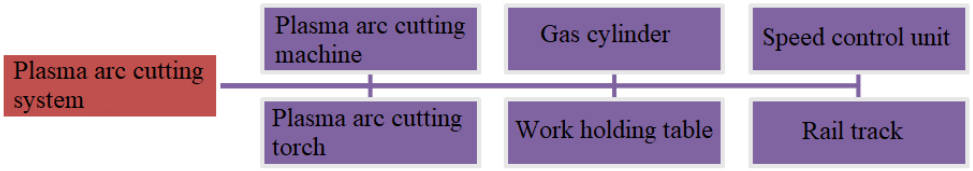

Figure 1. Experimental setup of plasma arc cutting system

Table 1. Experimental data samples [12]

Input 1 Cutting Current, A	**Input 2** Cutting Speed, mm/s	**Input 3** Gas Pressure, 1/min	**Input 4** Stand-off Gap, mm	**Output 1** MRR, mm^2/min	**Output 2** Surface Roughness, lm	**Output 3** Chamfer, mm	**Output 4** Dross, mm^2	**Output 5** Kerf width, mm	**Output 6** HAZ mm
100	2	15	2.5	1056.12	21.7	0.24	1.38	2.78	1.53
200	2	15	2.5	733.27	18.23	0.21	1.12	2.66	2.4
100	4	15	2.5	1049.5	23	0.31	1.36	2.75	2.02
200	4	15	2.5	890.65	19.96	0.22	1.3	2.7	1.86
150	3	12	2	979.92	20.88	0.22	1.36	2.68	1.79
150	3	18	2	1219.03	23.63	0.29	1.47	2.86	1.69
150	3	12	3	931.24	20	0.21	1.29	2.75	2.03
150	3	18	3	880.36	18.98	0.19	1.26	2.64	2.11
100	3	15	2	1270.86	25.85	0.32	1.57	2.87	1.34
200	3	15	2	1087.42	23.69	0.3	1.4	2.79	1.84
100	3	15	3	1134.58	24.19	0.31	1.41	2.8	1.82
200	3	15	3	836.33	19.83	0.21	1.28	2.71	2.02
150	2	12	2.5	609.54	15.77	0.14	1.07	2.61	2.2
150	4	12	2.5	1001.8	19.77	0.22	1.34	2.69	2.01
150	2	18	2.5	1020.53	19.12	0.21	1.3	2.72	2.03
150	4	18	2.5	779.04	18.15	0.2	1.19	2.65	2.16
100	3	12	2.5	948.27	20.55	0.24	1.32	2.71	1.95
200	3	12	2.5	865.77	19.64	0.21	1.27	2.7	1.87
100	3	18	2.5	1200.73	23.76	0.29	1.47	2.82	1.51
200	3	18	2.5	801.54	18.15	0.21	1.2	2.65	2.29
150	2	15	2	1367.02	25.37	0.34	1.56	2.85	1.5
150	4	15	2	788.54	19.53	0.2	1.22	2.7	2.07
150	2	15	3	519.48	15.26	0.11	1	2.62	2.43
150	4	15	3	1248.72	24.13	0.32	1.5	2.79	1.8
150	3	15	2.5	773.53	17.38	0.15	1.23	2.57	2.13
150	3	15	2.5	773.61	17.39	0.16	1.25	2.56	2.13
150	3	15	2.5	773.33	17.38	0.16	1.22	2.55	2.12

2.2 ANFIS Methodology

Figure 2 depicts the five distinct layers of the ANFIS network. Within the ANFIS framework, the fuzzy inference system functions analogously to a central nervous system. The first layer receives inputs and employs membership functions to convert them into fuzzy values. For this study, the bell-shaped membership function was selected due to its superior efficacy in handling nonlinear data regression.

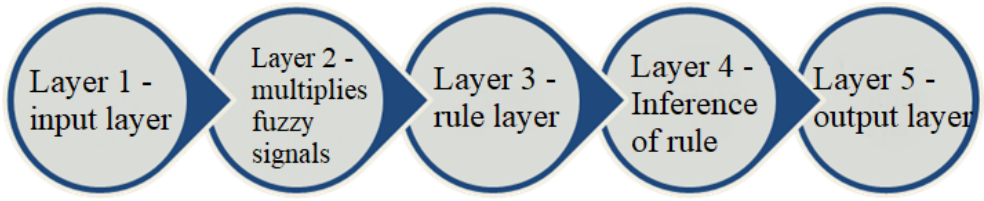

Figure 2. ANFIS layers

The membership functions, characterized by a bell-shape, are defined in the following manner:

$$\mu(x) = \text{bell}\,(x; a_i, b_i, c_i) = \frac{1}{1 + \left[\left(\frac{x - c_i}{a_i}\right)^2\right]^{b_i}} \tag{1}$$

where, $\{a_i, b_i, c_i\}$ denote the parameters set, while x is the input.

The calculation of rule firing strength involves multiplying the fuzzy signals generated by the first layer within the second layer. The third layer, known as the rule layer, is responsible for normalizing the signals emanating from the second layer. The fourth layer undertakes the task of rule inference and transforms all signals into crisp values. The final layer produces an impeccable output through the aggregation of all incoming signals.

3 Results

By employing the ANFIS approach, the most precise predictors for each type of defect were identified. The process of selecting and preprocessing input parameters to remove extraneous information is critical. The MATLAB command below is used to split the dataset into a training set (odd-indexed samples) and a checking set (even-indexed samples):

```
>>[data] = plasma;

>> trn_data = data(1:2:end,:);

>> chk_data = data(2:2:end,:);
```

The function "exhsrch" determines the set of inputs that have the greatest impact on the six output variables through an exhaustive search of all available inputs. The first argument of the function specifies the number of input combinations to be evaluated during the selection process. "Exhsrch" first constructs an ANFIS model for all possible combinations. The model is then trained for a single epoch, after which the outcomes are evaluated. The command line used to identify the one and two most important factors in predicting outputs is as follows:

```
>> exhsrch(1,trn_data,chk_data);

>> exhsrch(2,trn_data,chk_data);
```

Table 2. Correlation matrix of the one- and two-attributes influence on the recycling rate

MRR	Cutting Current, A	Cutting Speed, mm/s	Gas Pressure, 1/min	Stand-off Gap, mm
Cutting Current, A	trn = 200.4070 chk = 266.0967			
Cutting Speed, mm/s	trn = 198.5691, chk = 265.8494	trn = 227.9316, chk = 185.7137		
Gas Pressure, 1/min	trn = 189.1326, chk = 270.5929	trn = 200.4373, chk = 413.1904	trn = 218.9203, chk = 206.6505	
Stand-off Gap, mm	trn = 140.9772, chk = 310.8652	trn = 148.4954, chk = 197.2559	trn = 157.0890, chk = 282.0749	trn = 196.6478, chk = 186.2681

Table 2 displays the correlations between the effects of single and dual input combinations on the Material Removal Rate (MRR). These effects are quantified using the Root Mean Square Error (RMSE) for both training and error checking. The standoff distance has the most significant impact on the MRR and is associated with the smallest

training error. Essentially, even minor adjustments to the standoff distance can lead to considerable changes in the MRR.

When combining the cutting current and standoff distance, the training error decreases further, which indicates a greater influence on the MRR. Conversely, the most significant variation in MRR is expected to occur with simultaneous changes to the cutting current and standoff distance. Figure 3 illustrates the ANFIS decision surface generated by using the two optimal inputs.

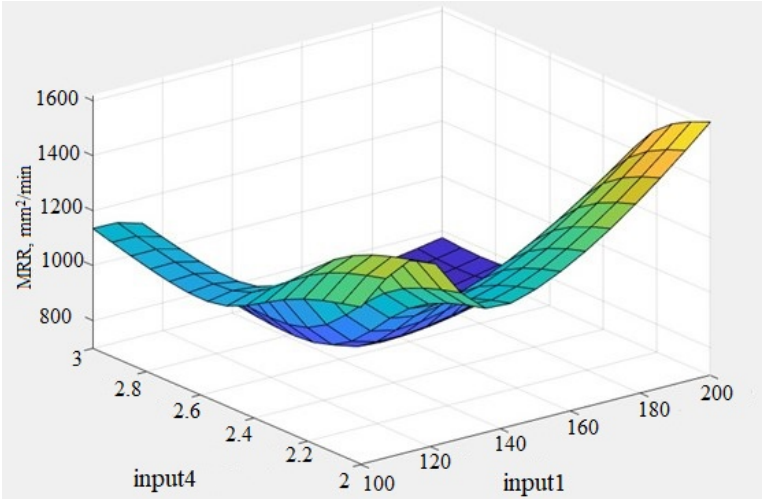

Figure 3. Optimal ANFIS decision surface for MRR

Table 3. Correlation matrix between input parameters and surface roughness

Surface Roughness	Cutting Current, A	Cutting Speed, mm / s	Gas Pressure, 1 / min	Stand-off Gap, mm
Cutting Current, A	trn = 2.5681, chk = 4.3947			
Cutting Speed, mm/s	trn = 2.5276, chk = 4.4007	trn = 3.1573, chk = 2.8265		
Gas Pressure, 1/min	trn = 2.4495, chk = 4.3424	trn = 2.8351, chk = 6.6431	trn = 3.2032, chk = 2.4485	
Stand-off Gap, mm	trn = 1.5345, chk = 4.5983	trn = 2.1837, chk = 3.4789	trn = 2.5032, chk = 3.3776	trn = 2.8467, chk = 2.0403

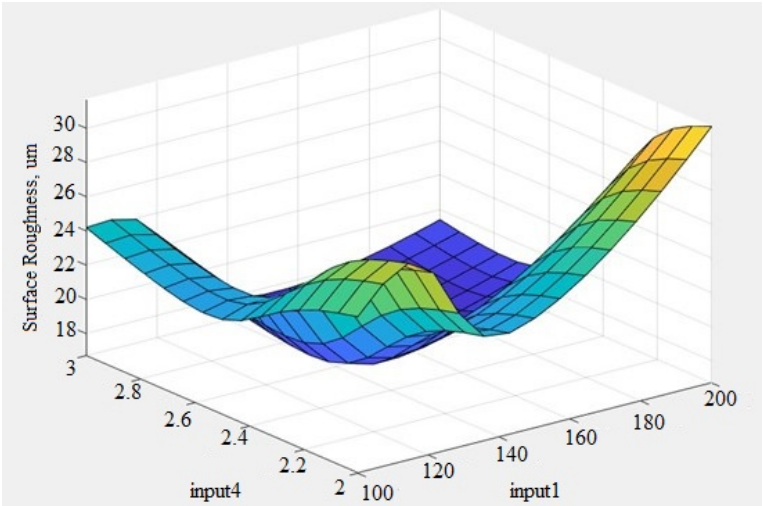

Figure 4. Optimal ANFIS decision surface for surface roughness

Table 3 shows the relationships between the effects of single and combined input pairs on surface roughness. Among the input parameters, the cutting current exerts the greatest influence on surface roughness, as indicated by its status as the most accurate during training. In other words, even minimal adjustments to the cutting current can lead to significant variations in surface roughness.

The pairing of cutting current and standoff distance significantly affects surface roughness by reducing the training error. Specifically, alterations in surface roughness are most pronounced when both the cutting current and standoff distance are varied together. Figure 4 presents the ANFIS decision surface generated by employing the two most effective inputs.

Table 4 illustrates the relationships between the effects of single and paired input combinations on chamfer. The cutting current is the input parameter that most significantly influences the chamfer, as indicated by the least training error. Essentially, even small fluctuations in the cutting current can lead to considerable variations in the chamfer.

Combining the cutting current with the standoff distance minimizes the training error, which in turn exerts the most significant effect on the chamfer. More specifically, the chamfer is likely to show the greatest variation when changes in the cutting current and standoff distance occur simultaneously. Figure 5 shows the ANFIS decision surface that is derived from using the two optimal inputs.

Table 4. Correlation matrix between input parameters and chamfer

Chamfer	Cutting Current, A	Cutting Speed, mm / s	Gas Pressure, 1 / min	Stand-off Gap, mm
Cutting Current, A	$\mathrm{trn} = 0.0548$, $\mathrm{chk} = 0.0558$			
Cutting Speed, mm/s	$\mathrm{trn} = 0.0527$, $\mathrm{chk} = 0.0625$	$\mathrm{trn} = 0.0667$, $\mathrm{chk} = 0.0666$		
Gas Pressure, 1/min	$\mathrm{trn} = 0.0530$, $\mathrm{chk} = 0.0548$	$\mathrm{trn} = 0.0614$, $\mathrm{chk} = 0.1303$	$\mathrm{trn} = 0.0689$, $\mathrm{chk} = 0.0482$	
Stand-off Gap, mm	$\mathrm{trn} = 0.0367$, $\mathrm{chk} = 0.0739$	$\mathrm{trn} = 0.0453$, $\mathrm{chk} = 0.0871$	$\mathrm{trn} = 0.0569$, $\mathrm{chk} = 0.0834$	$\mathrm{trn} = 0.0638$, $\mathrm{chk} = 0.0439$

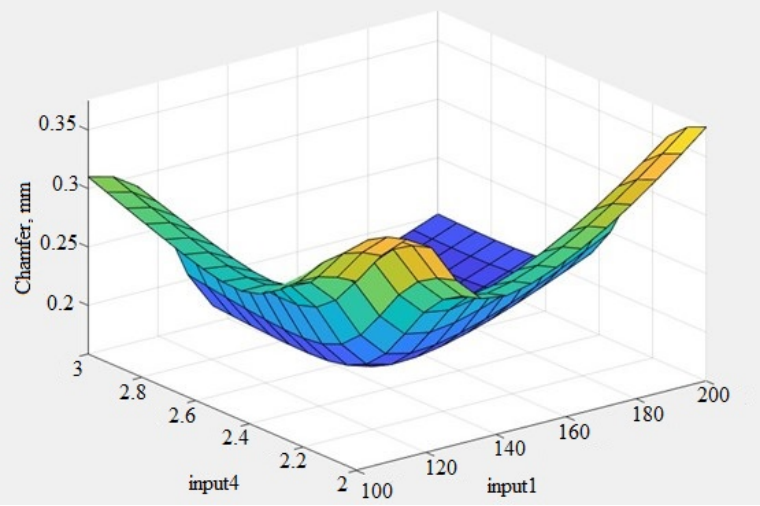

Figure 5. Optimal ANFIS decision surface for chamfer

Table 5 outlines the correlations between the effects of individual and combined input pairs on dross. The standoff gap, as an input feature, has the most profound impact on dross, associated with the least training error. Essentially, even minor adjustments to the standoff distance can lead to significant changes in dross.

When the cutting current and standoff distance are paired, there is a reduction in training error, which translates to a more substantial effect on dross. In practice, the most notable change in dross would occur when there are concurrent variations in both the cutting current and standoff gap. Figure 6 shows the ANFIS decision surface generated by employing the two optimal inputs.

Table 6 displays the relationships between the effects of single and combined input pairs on kerf width. The kerf width is most significantly influenced by the cutting current, which is the input parameter with the lowest training error. Essentially, even minor fluctuations in the cutting current can lead to considerable shifts in kerf width.

Table 5. Correlation matrix between input parameters and dross

Dross	Cutting Current, A	Cutting Speed, mm / s	Gas Pressure, 1 / min	Stand-off Gap, mm
Cutting Current, A	trn = 0.1333 chk = 0.3058			
Cutting Speed, mm/s	trn = 0.1303, chk = 0.3174	trn = 0.1491, chk = 0.1134		
Gas Pressure, 1/min	trn = 0.1290 chk = 0.3054	trn = 0.1334 chk = 0.2615	trn = 0.1501, chk = 0.1264	
Stand-off Gap, mm	trn = 0.0855, chk = 0.3197	trn = 0.0931 chk = 0.1117	trn = 0.1039, chk = 0.1768	trn = 0.1254, chk = 0.1286

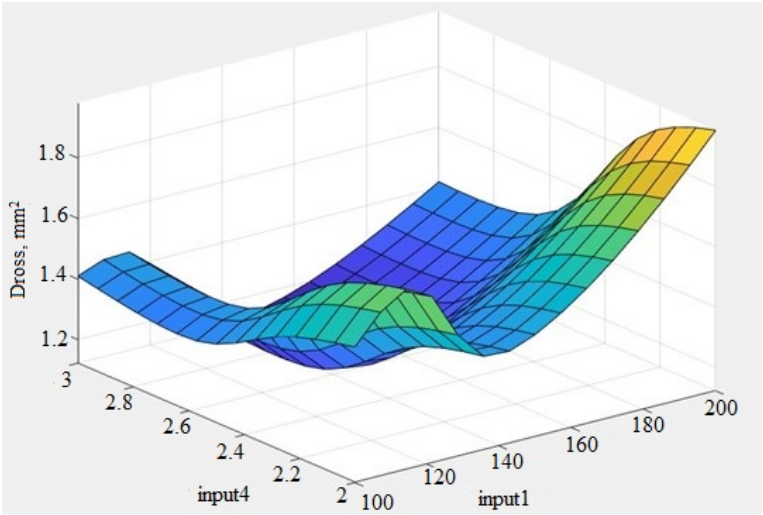

Figure 6. Paternoster transport solutions for unloading (roller and belt conveyor)

The combination of cutting current and standoff distance reduces the training error, thereby having the most pronounced influence on kerf width. Practically speaking, the kerf width would experience the greatest variation when changes to the cutting current and standoff gap occur concurrently. Figure 7 illustrates the ANFIS decision surface created by utilizing the two optimal inputs.

Table 6. Correlation matrix between input parameters and kerf width

Kerf Width	Cutting Current, A	Cutting Speed, mm / s	Gas Pressure, 1 / min	Stand-off Gap, mm
Cutting Current, A	trn = 0.0790, chk = 0.5970			
Cutting Speed, mm/s	trn = 0.0744, chk = 0.5748	trn = 0.0983, chk = 0.0808		
Gas Pressure, 1/min	trn = 0.0731, chk = 0.5837	trn = 0.0881, chk = 0.1919	trn = 0.0953, chk = 0.0855	
Stand-off Gap, mm	trn = 0.0577, chk = 0.5746	trn = 0.0767 chk = 0.1121	trn = 0.0702, chk = 0.1311	trn = 0.0884, chk = 0.0594

Table 7 shows the correlations between the effects of individual and combined input pairs on the Heat-Affected Zone (HAZ). The standoff distance is the input parameter that has the most substantial impact on the HAZ, as evidenced by the smallest training error. Essentially, even minor adjustments to the standoff distance can lead to significant changes in the HAZ.

The combination of cutting current and standoff gap minimizes the training error and, therefore, has the most profound influence on the HAZ. Put another way, the HAZ would undergo the greatest degree of variation when the cutting current and standoff distance are altered simultaneously. Figure 8 depicts the ANFIS decision surface generated using the two optimal inputs.

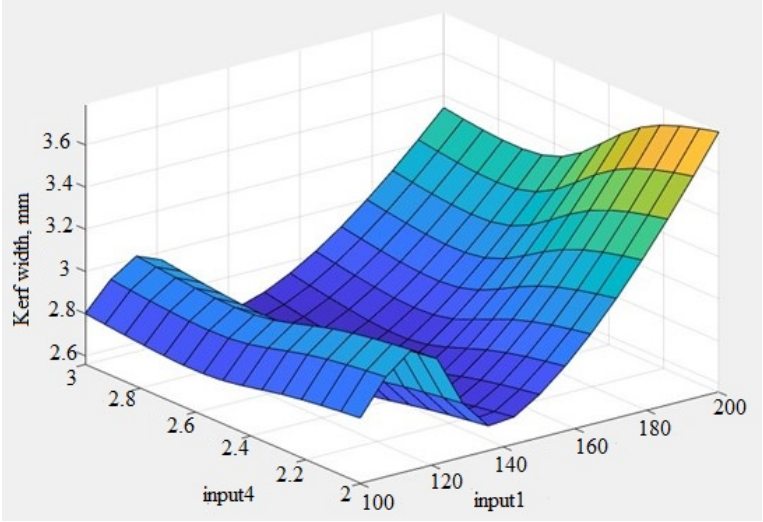

Figure 7. Scheme of a rectangular conveyor

Table 7. Correlation matrix between input parameters and HAZ

HAZ	Cutting Current, A	Cutting Speed, mm / s	Gas Pressure, 1 / min	Stand-off Gap, mm
Cutting Current, A	trn = 0.2562, chk = 0.4912			
Cutting Speed, mm/s	trn = 0.2359, chk = 0.4818	trn = 0.2988 chk = 0.2375		
Gas Pressure, 1/min	trn = 0.2415, chk = 0.4920	trn = 0.2674, chk = 0.6201	trn = 0.2957, chk = 0.2767	
Stand-off Gap, mm	trn = 0.1594, chk = 0.5895	trn = 0.2102, chk = 0.3228	trn = 0.2084, chk = 0.3930	trn = 0.2390 chk = 0.2663

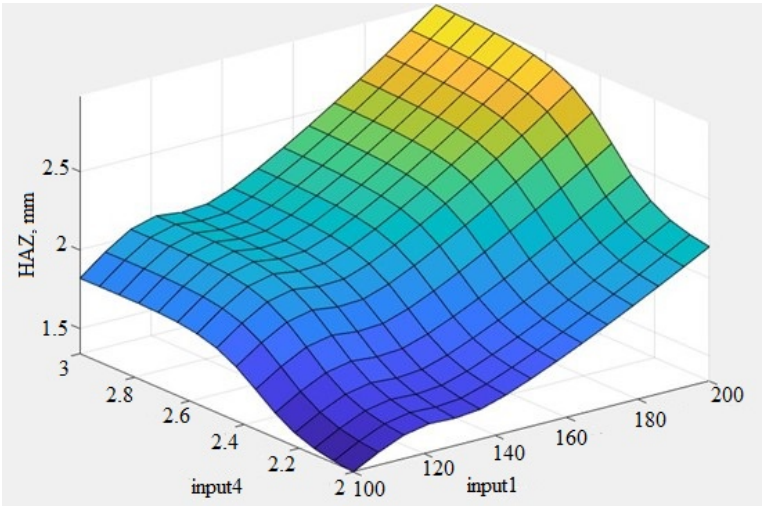

Figure 8. Optimal ANFIS decision surface for HAZ

4 Conclusions

In the industrial sector, plasma arc cutting is utilized for particularly demanding tasks. Traditional control methods fall short due to the complex nature of the input parameters, rendering them unsuitable for advancing technology in this area. This experiment employed a data-driven optimization approach to enhance the plasma arc cutting process. The quality of the cut is evaluated by six output attributes. The input factors are classified as the standoff gap, cutting current, and cutting speed. The output variables include the Material Removal Rate (MRR),

surface roughness, chamfer, dross, kerf width, and Heat-Affected Zone (HAZ).

The primary goal of this research was to identify the most significant characteristics that determine the most effective settings for plasma arc cutting. An adaptive neural fuzzy inference system (ANFIS) was employed to analyze the various input parameters of the plasma arc cutting process. According to ANFIS predictions, the variables of Material Removal Rate (MRR), chamfer, surface roughness, dross, kerf width, and Heat-Affected Zone (HAZ) are most significantly influenced by the combination of cutting current and standoff distance. In other words, the optimal configuration for predicting the dimensions of the Heat-Affected Zone, Material Removal Rate (MRR), surface roughness, chamfer, dross, and kerf width occurs when the cutting current and standoff gap are considered in tandem.

Data Availability

The data used to support the research findings are available from the corresponding author upon request.

Conflicts of Interest

The authors declare no conflict of interest.

References

[1] D. N. Sharma and J. R. Kumar, "Optimization of dross formation rate in plasma arc cutting process by response surface method," *Mater. Today Proc.*, vol. 32, pp. 354–357, 2020. https://doi.org/10.1016/j.matpr.2020.01.605

[2] A. Rajeshkannan, M. Ali, R. Prakash, R. Prasad, A. K. Jeevanantham, and K. Jayaram, "Optimizing the process parameters in plasma arc cutting using taguchi approach for the case industry in Fiji," *Mater. Today Proc.*, vol. 24, no. 2, pp. 1122–1131, 2020. https://doi.org/10.1016/j.matpr.2020.04.425

[3] D. Singh and Y. Shrivastava, "Identification of suitable machining zone during the plasma arc cutting of SS-304," *Mater. Today Proc.*, vol. 38, pp. 413–417, 2021. https://doi.org/10.1016/j.matpr.2020.07.598

[4] A. Suresh and G. Diwakar, "Optimization of process parameters in plasma arc cutting for TWIP steel plates," *Mater. Today Proc.*, vol. 38, no. 5, pp. 2417–2424, 2021. https://doi.org/10.1016/j.matpr.2020.07.383

[5] K. Ananthakumar, D. Rajamani, E. Balasubramanian, and J. P. Davim, "Measurement and optimization of multi-response characteristics in plasma arc cutting of Monel 400™ using RSM and TOPSIS," *Meas.*, vol. 135, pp. 725–737, 2019. https://doi.org/10.1016/j.measurement.2018.12.010

[6] J. Deli and Y. Bo, "An intelligent control strategy for plasma arc cutting technology," *J. Manuf. Process.*, vol. 13, no. 1, pp. 1–7, 2011. https://doi.org/10.1016/j.jmapro.2010.08.003

[7] K. D. Naik and K. P. Maity, "An optimization and experimental analysis of plasma arc cutting of hardox-400 using taguchi based desirability analysis," *Mater. Today Proc.*, vol. 5, no. 5, pp. 13 157–13 165, 2018. https://doi.org/10.1016/j.matpr.2018.02.306

[8] J. S. Jang, "ANFIS: Adaptive-network-based fuzzy inference system," *IEEE Trans. Syst., Man, Cybern.*, vol. 23, no. 3, pp. 665–685, 1993. https://doi.org/10.1109/21.256541

[9] S. R. Mangaraj, D. K. Bagal, N. Parhi, S. N. Panda, A. Barua, and S. Jeet, "Experimental study of a portable plasma arc cutting system using hybrid rsm-nature inspired optimization technique," *Mater. Today Proc.*, vol. 50, no. 5, pp. 867–878, 2022. https://doi.org/10.1016/j.matpr.2021.06.138

[10] J. Deli and Y. Bo, "An intelligent control strategy for plasma arc cutting technology," *J. Manuf. Process.*, vol. 13, no. 1, pp. 1–7, 2011. https://doi.org/10.1016/j.jmapro.2010.08.003

[11] C. Prakash, S. Singh, M. Singh, K. Verma, B. Chaudhary, and S. Singh, "Multi-objective particle swarm optimization of EDM parameters to deposit HA-coating on biodegradable Mg-alloy," *Vacuum*, vol. 158, pp. 180–190, 2018. https://doi.org/10.1016/j.vacuum.2018.09.050

[12] A. Babbar, C. Prakash, S. Singh, M. K. Gupta, M. Mia, and C. I. Pruncu, "Application of hybrid nature-inspired algorithm: single and bi-objective constrained optimization of magnetic abrasive finishing process parameters," *J. Mater. Res. Technol.*, vol. 9, no. 4, pp. 7961–7974, 2020. https://doi.org/10.1016/j.jmrt.2020.05.003

[13] S. Mirjalili and A. Lewis, "The whale optimization algorithm," *Adv. Eng. Softw.*, vol. 95, p. 51, 2016. https://doi.org/10.1016/j.advengsoft.2016.01.008

[14] F. B. Ozsoydan, "Effects of dominant wolves in grey wolf optimization algorithm," *Appl. Soft Comput.*, vol. 83, p. 105658, 2019. https://doi.org/10.1016/j.asoc.2019.105658

[15] M. R. Shakarami and I. F. Davoudkhani, "Wide-area power system stabilizer design based on grey wolf optimization algorithm considering the time delay," *Electr. Power Syst. Res.*, vol. 133, p. 149, 2016. https://doi.org/10.1016/j.epsr.2015.12.019

[16] R. V. Rao, K. More, J. Taler, and P. Oc loń, "Dimensional optimization of a micro-channel heat sink using jaya algorithm," *Appl. Therm. Eng.*, vol. 103, p. 572, 2016. https://doi.org/10.1016/j.applthermaleng.2016.04.135